

A two-photon fluorescent RNA probe screened from a series of oxime-functionalized 2,2':6',2''-terpyridine ZnX₂ (X = Cl, Br, I) complexes

Hui Wang^a, Xiaohe Tian^{*b}, Wei Du^a, Qiong Zhang^a, Aidong Wang^c, Yujin Zhang^d, Chuankui Wang^d, Lijuan Guan^e, Hongping Zhou^a, Jieying Wu^{*a}, Yupeng Tian^{a,f}

[a] Department of Chemistry, Key Laboratory of Functional Inorganic Material Chemistry of Anhui Province, Anhui University, Hefei 230601, P. R. China

[b] School of Life Science, Anhui University, Hefei 230601, P.R. China

[c] Huangshan University, Huangshan, China

[d] College of Physics and Electronics, Shandong Normal University, Jinan 250014, China

[e] Department of Chemistry, University College London, WC1H0AJ, UK

[f] State Key Laboratory of Coordination Chemistry, Nanjing University, Nanjing 210093, P. R. China

*Corresponding author. Tel: +86-551-63861227

E-mail address: t.xiaohe@ucl.ac.uk; jywu1957@163.com

Experiment section	S3
Measurements and apparatus	S3
Optical measurements	S3
Synthesis	S4
X-ray crystallography	S5
Computational details	S7
Cell Imaging	S7
Two-photon microscopy	S8
Cytotoxicity assays in cells	S8
Table S1. Crystal data collection and structure refinement of OTP, FTP-ZnCl₂, FTP-ZnBr₂, OTP-ZnCl₂, OTP-ZnBr₂ and OTP-ZnI₂	S8
Table S2. Selected bond lengths (Å) and angles (°) of OTP	S9
Table S3. Selected bond lengths (Å) and angles (°) of FTP-ZnCl₂	S9
Table S4. Selected bond lengths (Å) and angles (°) of FTP-ZnBr₂	S9

Table S5. Selected bond lengths (Å) and angles (°) of OTP-ZnCl₂	S9
Table S6. Selected bond lengths (Å) and angles (°) of OTP-ZnBr₂	S10
Table S7. Selected bond lengths (Å) and angles (°) of OTP-ZnI₂	S10
Fig S1. Linear absorption spectra of OTP , FTP-ZnX₂ and OTP-ZnX₂ (X=Cl, Br, I) in different solvents (c=10 μM).....	S11
Table S8. The photophysical data of OTP , FTP-ZnX₂ and OTP-ZnX₂ (X=Cl, Br, I) in different solvents.....	S11
Fig S2. One-photon fluorescence spectra of OTP , FTP-ZnX₂ and OTP-ZnX₂ (X=Cl, Br, I) in different solvents (c=10 μM).....	S13
Fig S3. Molecular orbital energy diagram of OTP	S13
Fig S4. Molecular orbital energy diagram of FTP-ZnCl₂ (left) and OTP-ZnCl₂ (right).....	S14
Fig S5. Molecular orbital energy diagram of FTP-ZnBr₂ (left) and OTP-ZnBr₂ (right).....	S14
Fig S6. Molecular orbital energy diagram of FTP-ZnI₂ (left) and OTP-ZnI₂ (right).....	S14
Table S9. Calculated linear absorption properties (nm), excitation energy (eV), oscillator strengths and major contribution for all compounds.....	S15
Fig S7. Lippert-Mataga plots for FTP , OTP , FTP-ZnX₂ and OTP-ZnX₂ (X=Cl, Br, I).....	S15
Fig S8. Cytotoxicity data results obtained from the MTT assay.....	S16
Fig S9. One- and two-photon images of HepG2 cells incubated with FTP , OTP and their ZnX ₂ (X=Cl, Br, I) complexes (30 μM, 30 min) at 37 °C. One-photon excited wavelength: 405 nm; emission filter: 510-570 nm. Two-photon excited wavelength: 820 nm; emission filter: 520-580 nm.....	S17
Fig S10. Two-photon imaging of A549, MCF-7 and 3T3 cells stained with 30 μM OTP-ZnCl₂ for 30 min.	S18
Fig S11. Two-photon image of HepG2 cells incubated with OTP-ZnCl₂ at 37 °C and 4 °C for 30 minutes.	S18
Fig S12. HepG2 cells by flow cytometry upon incubating the cells with OTP-ZnCl₂ for 30 min before and after treatment with DNase and RNase for 2 h.....	S19
Fig S13. Live cell counterstain with Hoechst 33342. Two-photon imaging of HepG2 cells stained with OTP-ZnCl₂ (30 μM) (a) for 30 min followed by staining with 1 μM Hoechst 33342 (b) for 15 min. (c) Merge image of OTP-ZnCl₂ and Hoechst 33342. Scale bar= 20 μm.....	S19
Fig. S14 The view of the interaction between OTP-ZnCl₂ with RNA fragment.....	S20
Fig. S15 The view of the hydrogen bond interaction between OTP-ZnCl₂ and FTP-ZnCl₂ with the surface of RNA fragment (Aubergine represents FTP-ZnCl₂ , gray represents OTP-ZnCl₂).....	S20

Experiment section

Measurements and apparatus

All reagents were obtained commercially and used as supplied. Elemental analysis was performed with a Perkin-Elmer 240B instrument. ¹H-NMR and ¹³C-NMR spectra were obtained on a Bruker Avance 400 spectrometer (TMS as internal standard in NMR). MALDI-TOF mass spectra were recorded using a Bruker Autoflex III Smartbeam. Melting points were measured on a FP62 instrument. IR spectra were recorded on a NEXUS 870 (Nicolet) spectrophotometer in the 4000-400 cm⁻¹ range with samples prepared as KBr pellets.

Optical measurements

UV spectra were recorded on a UV-265 spectrophotometer. The fluorescence spectra were measured by using a HITACHI F-7000 fluorescence spectrophotometer. The concentration of a sample solution was 1.0×10⁻⁵ mol/L. The fluorescence quantum yields (Φ) were determined by using fluorescein as the reference according to the literature method [1]. Two-photon absorption (2PA) cross-sections of all compounds were obtained by the two-photon excited fluorescence (2PEF) method with femtosecond laser pulses and a Ti: sapphire system (680-1080 nm, 80 MHz, 140 fs) as the light source. The concentration of the sample solution was 5.0×10⁻⁴ mol/L. Thus, the σ values of samples were determined by the following equation:

$$\sigma = \sigma_{ref} \frac{\Phi_{ref} c_{ref} n_{ref} F}{\Phi c n F_{ref}}$$

where the subscripts ref stands for the reference molecule. σ is the 2PA cross-section value, c is the concentration of solution, n is the refractive index of the solution, F is the integrated area of the detected two-photon-induced fluorescence signal, and Φ is the fluorescence quantum yield. The σ_{ref} value of reference is taken from the literature [2-3].

For time-resolved fluorescence measurements, the fluorescence signals were collimated and focused onto the entrance slit of a monochromator with the output plane equipped with a photomultiplier tube (HORIBA HuoroMax-4P). The decays were analyzed by 'least-squares'. The quality of the exponential fits was evaluated by the goodness of fit (χ²).

Synthesis

Synthesis of OTP

A mixture of 0.078 g (0.155 mmol) **FTP** [4], 0.016 g (0.233 mmol) $\text{NH}_2\text{OH}\cdot\text{HCl}$, 0.024 g (0.233 mmol) Et_3N in ethanol, were heated to 80 °C for 3 h. After the reaction, the solvent was removed under reduced vacuum. The light yellow solid was appeared and filtered, which was washed with successively water, ethanol and dried under vacuum at 80 °C. Yield: 60%. M.p.: 255 °C. IR (KBr, cm^{-1}): 3060, 1594, 1583, 1510, 1467, 1390, 1323, 1280, 1181, 965, 837, 792, 697, 536, 519. $^1\text{H-NMR}$ (400 MHz, DMSO): 11.10 (s, 1H), 8.76 (d, 2H), 8.68 (m, 5H), 8.04 (m, 2H), 7.90 (d, 2H), 7.53 (m, 5H), 7.39 (t, 2H), 7.17 (m, 5H), 7.09 (d, 2H). $^{13}\text{C-NMR}$ (100 MHz, DMSO): 117.19, 120.88, 123.29, 123.54, 124.47, 125.27, 127.77, 128.04, 129.85, 131.07, 137.43, 146.29, 147.54, 149.30, 154.98, 155.60. MS: 519.60 ($[\text{M}]^+$). Anal. Calc. for $\text{C}_{34}\text{H}_{25}\text{N}_5\text{O}$: C, 78.59; H, 4.85; N, 13.48; Found: C, 78.65; H, 4.85; N, 13.46.

Synthesis of Zn(II) complexes

A solution of **FTP/OTP** (0.400 mmol) was dissolved in ethanol, followed by the dropwise addition of ZnX_2 (X=Cl, Br, I) (0.400 mmol) in 5 mL ethanol, and the reaction mixture was refluxed for 4 h. The mixture was cooled down to room temperature and filtered. The pure product was eventually recrystallized by ethanol.

FTP-ZnCl₂ : Yield: 87%. M.p. > 300 °C. IR (KBr, cm^{-1}): 3060, 2933, 2827, 2738, 1685, 1586, 1509, 1475, 1431, 1327, 1296, 1164, 1070, 1017, 829, 792, 696, 526. $^1\text{H-NMR}$ (400 MHz, d_6 -DMSO): 9.86 (s, 1H), 9.17 (s, 2H), 8.94 (d, 2H), 8.84 (s, 2H), 8.33 (m, 4H), 7.87 (m, 4H), 7.49 (t, 2H), 7.34 (m, 5H), 7.13(d, 2H). $^{13}\text{C-NMR}$ (100 MHz, d_6 -DMSO): 119.73, 120.39, 122.49, 124.95, 126.15, 126.69, 129.67, 130.22, 131.33, 140.53, 145.32, 148.72, 190.90. MS: 602.72 ($[\text{M-Cl}]^+$). Anal. Calc. for $\text{C}_{34}\text{H}_{24}\text{N}_4\text{OCl}_2\text{Zn}$: C, 63.72; H, 3.77; N, 8.74; Found: C, 63.77; H, 3.77; N, 8.73.

FTP-ZnBr₂ : Yield: 90%. M.p. > 300 °C. IR (KBr, cm^{-1}): 3058, 1684, 1588, 1507, 1473, 1430, 1324, 1294, 1162, 1015, 834, 790, 695, 519. $^1\text{H-NMR}$ (400 MHz, d_6 -DMSO): 9.86 (s, 1H), 9.09 (s, 2H), 8.96 (d, 4H), 8.34 (m, 4H), 7.90 (m, 4H), 7.50 (t, 2H), 7.35 (m, 5H), 7.13 (d, 2H). $^{13}\text{C-NMR}$ (100 MHz, d_6 -DMSO): 120.43, 124.90, 125.98, 126.71, 127.29, 129.71, 130.24, 131.34, 140.78, 145.30, 148.65, 151.97, 190.92. MS: 648.99 ($[\text{M-Br}]^+$). Anal. Calc. for $\text{C}_{34}\text{H}_{24}\text{N}_4\text{OBr}_2\text{Zn}$: C, 55.96; H, 3.31; N, 7.68; Found: C, 55.90; H, 3.31; N, 7.68.

FTP-ZnI₂ : Yield: 89%. M.p. > 300 °C. IR (KBr, cm⁻¹): 3059, 1684, 1516, 1505, 1490, 1473, 1428, 1296, 1249, 1221, 1166, 1020, 830, 790, 538, 525. ¹H-NMR (400 MHz, d₆-DMSO): 9.89 (d, 1H), 9.36 (s, 1H), 9.13 (s, 1H), 9.05 (d, 1H), 8.95 (d, 1H), 8.44 (m, 2H), 8.31 (d, 2H), 7.95 (d, 2H), 7.87 (t, 2H), 7.51 (m, 4H), 7.35 (m, 4H), 7.16 (m, 2H). ¹³C-NMR (100 MHz, d₆-DMSO): 120.43, 123.49, 124.91, 126.75, 129.90, 130.26, 131.36, 141.29, 145.30, 151.96, 190.93. MS: 694.97 ([M-I]⁺). Anal. Calc. for C₃₄H₂₄N₄OI₂Zn: C, 49.57; H, 2.94; N, 6.80; Found: C, 49.61; H, 2.94; N, 6.80.

OTP-ZnCl₂ : Yield: 88%. M.p. > 300 °C. IR (KBr, cm⁻¹): 3061, 2959, 1590, 1513, 1474, 1328, 1203, 1020, 963, 829, 793, 695, 518. ¹H NMR (400 MHz, d₆-DMSO): 11.15 (s, 1H), 8.96 (s, 2H), 8.87 (d, 4H), 8.28 (s, 2H), 8.17 (d, 2H), 7.83 (s, 2H), 7.60 (d, 2H), 7.43 (m, 2H), 7.19 (m, 8H). ¹³C-NMR (100 MHz, d₆-DMSO): 119.13, 122.38, 124.06, 125.61, 127.78, 128.34, 129.31, 129.94, 140.45, 145.97, 147.12, 148.70, 149.31, 153.43. MS: 620.87 ([M-Cl]⁺). Anal. Calc. for C₃₄H₂₅N₅OCl₂Zn: C, 62.26; H, 3.84; N, 10.68; Found: C, 62.20; H, 3.84; N, 10.69.

OTP-ZnBr₂ : Yield: 91%. M.p. > 300 °C. IR (KBr, cm⁻¹): 3056, 2859, 1592, 1510, 1473, 1368, 1285, 1179, 1016, 959, 831, 793, 730, 526. ¹H NMR (400 MHz, d₆-DMSO): 11.15 (s, 1H), 9.05 (s, 2H), 8.95 (d, 4H), 8.36 (t, 2H), 8.21 (d, 2H), 8.12 (s, 1H), 7.90 (s, 2H), 7.61 (d, 2H), 7.43 (t, 2H), 7.18 (m, 7H). ¹³C-NMR (100 MHz, d₆-DMSO): 119.25, 122.06, 124.10, 125.63, 127.79, 129.39, 129.96, 140.64, 145.96, 147.11, 148.56, 149.38, 153.59. MS: 664.16 ([M-Br]⁺). Anal. Calc. for C₃₄H₂₅N₅OBr₂Zn: C, 54.83; H, 3.38; N, 9.40; Found: C, 54.88; H, 3.38; N, 9.41.

OTP-ZnI₂ : Yield: 90%. M.p. > 300 °C. IR (KBr, cm⁻¹): 3055, 1588, 1511, 1487, 1472, 1410, 1326, 1247, 1183, 1014, 955, 829, 791, 729, 697, 522. ¹H NMR (400 MHz, d₆-DMSO): 11.17 (s, 1H), 9.31 (s, 1H), 9.12 (d, 3H), 8.93 (s, 1H), 8.35 (m, 4H), 8.15 (s, 1H), 7.93 (s, 2H), 7.62 (t, 2H), 7.49 (t, 3H), 7.23 (m, 7H). ¹³C-NMR (100 MHz, d₆-DMSO): 120.03, 122.61, 124.76, 126.21, 128.31, 129.99, 130.51, 141.75, 146.45, 147.59, 147.97. MS: 709.94 ([M-I]⁺). Anal. Calc. for C₃₄H₂₅N₅OI₂Zn: C, 48.68; H, 3.00; N, 8.35; Found: C, 48.72; H, 3.00; N, 8.34.

X-ray crystallography

The X-ray diffraction measurements were performed on a Bruker SMART CCD area detector using graphite monochromated Mo-K_α radiation ($\lambda = 0.71069 \text{ \AA}$) at 298(2)K. Intensity data were collected in the variable ω -scan mode. The structures were solved by direct methods and difference Fourier transformations. The non-hydrogen atoms were refined anisotropically and

hydrogen atoms were introduced geometrically. Calculations were performed with SHELXTL-97 program package [5].

Computational details

Optimizations were carried out with B3LYP [LANL2DZ] without any symmetry restraints, and the TD-DFT {B3LYP[LANL2DZ]} calculations were performed on the optimized structure. All calculations, including optimizations and TD-DFT, were performed with the G03 software [6]. Geometry optimization of the singlet ground state and the TD-DFT calculation of the lowest 25 singlet-singlet excitation energies were calculated with a basis set composed of 6-31G* for C H N O atoms and the Lanl2dz basis set for Zn, Cl, Br and I atoms were download from the EMSL basis set library.

Cell Imaging

HepG2, A549, MCF-7 and 3T3 cells were seeded in 24-well glass bottom plates at a density of 1×10^4 cells per well and grown for 96 hours. For live cell imaging, cells were incubated with the complexes at 30 μM in cell medium containing 10% Fetal Bovine Serum (FBS) and maintained at 37°C in an atmosphere of 5% CO₂ and 95% air for 30 min. The cells were then washed with PBS three times. The cells were imaged using water immersion lenses on a confocal laser scanning microscopy. Co-staining was performed using 3 μM Syto9 for 20 min and 1 μM Hoechst 33342 for 15 min.

For DNase and RNase digestion test, three sets of pretreated HepG2 cells were stained with 30 μM **OTP-ZnCl₂** for 30 min. A total of 1 mL clean PBS (as the control experiment), 30 $\mu\text{g mL}^{-1}$ DNase I, or 25 $\mu\text{g mL}^{-1}$ RNase A was added into the three adjacent wells and incubated at 37 °C in 5% CO₂ for 2 h. Cells were rinsed with clean PBS twice before imaging. For each dyeing test, the fluorescence images were obtained with an equal parameter for the control. In addition, the DNase and RNase digest tests of cells stained with 30 μM **OTP-ZnCl₂** was also carried out for comparison. Flow cytometry measurements were conducted using Beckman Gallios (USA) with excitation at 405 nm. The mean fluorescence was determined by counting 5000 events.

For transmission electron microscopy (TEM), HepG2 cells were incubated with complex **OTP-ZnCl₂** (30 min) then fixed in 3% glutaraldehyde and dehydrated in ethanol. TEM samples were sectioned in Araldite resin by microtome and examined on a FEI Tecnai instrument operating at 80 kV equipped with a Gatan 1 k CCD Camera.

Two-photon microscopy

Luminescent HepG2 cells were imaged with a Zeiss LSM 710 META upright confocal laser scanning microscope using magnification 60× objective lenses for monolayer cultures. Image data acquisition and processing were performed using Zeiss LSM Image Browser, Zeiss LSM Image Expert and Image J.

Cytotoxicity assays in cells

The cytotoxicity of all compounds was evaluated using the MTT assay. HepG2, MCF-7, A549 and 3T3 cells were seeded in 96-well plates at a density of 5000 cells/well and incubated for 2 days at 37 °C under 5 % CO₂. All compounds were then added at indicated concentrations to triplicate wells. Prior to the compounds' treatment, cell culture medium was changed, and aliquots of the compounds stock solutions were diluted to obtain the final concentrations of 5, 10, 20, 40 and 60 μM in growth medium. To ensure the same volume of compound solution to be added into each well with desired different concentrations, we started with different stock solutions. However, DMSO was controlled below 1% in the medium to minimize its effects on live cell imaging. For example, the higher trace of DMSO was present in 5 μM treatment group. To gain 5 μM working concentration, 1 mM stock solution (in DMSO) was first 1:10 (V:V) diluted in DMEM medium and further diluted 1:20 in DMEM medium. After incubation for 6 h, the medium was replaced with fresh DMEM medium. Subsequently, cells were treated with 5 mg/mL MTT (10 μL/well) and incubated for an additional 4 h (37 °C, 5% CO₂). After MTT medium removal, the formazan crystals were dissolved in DMSO (100 μL/well) and the absorbance was measured at 450 nm using a microplate reader (SpectraMax Paradigm).

Table S1. Crystal data collection and structure refinement of **OTP, FTP-ZnCl₂, FTP-ZnBr₂, OTP-ZnCl₂, OTP-ZnBr₂ and OTP-ZnI₂.**

Compound	OTP	FTP-ZnCl ₂	FTP-ZnBr ₂	OTP-ZnCl ₂	OTP-ZnBr ₂	OTP-ZnI ₂
Empirical formula	C ₃₄ H ₂₅ N ₅ O	C ₃₆ H ₂₇ N ₅ OCl ₂ Z n	C ₃₆ H ₂₇ N ₅ OZnB r ₂	C ₃₆ H ₂₅ N ₆ OZnC l ₂	C ₃₅ H ₂₇ N ₅ OZnBr ₂ C l ₂	C ₃₆ H ₂₇ N ₆ O ₂ ZnI ₂ C l ₂
CCDC	1455554	1455559	1455558	1455556	1455555	1455557
Formula weight	519.59	681.90	770.82	693.89	829.71	965.71
Crystal system, space group	Triclinic, Pī	Monoclinic, P2 ₁ /n	Triclinic, Pī	Monoclinic, P2 ₁ /c	Monoclinic, P2 ₁ /c	Monoclinic, P2 ₁ /c

Unit cell dimensions (Å ³)	A=8.894(2) b=10.241(2) c=15.811(2) α=79.530(2) β=86.870(2) γ=70.650(2)	a=14.796(5) b=14.776(5) c=16.532(5) β=114.555(5)	a=11.759(5) b=12.636(5) c=13.141(5) α=100.106(5) β=103.238(5) γ=114.716(5)	a=11.124(5) b=14.265(5) c=20.970(5) β=92.901(5)	a=11.057(5) b=14.625(5) c=21.079(5) β=91.805(5)	a=11.166(4) b=14.692(5) c=21.336(8) β=91.616(5)
Volume/ Å ³	1336 (4)	3287(2)	1643(1)	3323(2)	3407(2)	3499(2)
Z, Calculated density/Mg m ³	2, 1.292	4, 1.378	2, 1.558	4, 1.387	4, 1.618	4, 1.682
Absorption coefficient/mm ⁻¹	0.080	0.946	3.216	0.938	3.260	2.578
F(000)	544	1400	772	1420	1656	1722
Goodness-of-fit on F ²	1.093	1.011	0.963	0.984	1.090	1.000
Final R indices [I>2σ]	R ₁ =0.0789, wR ₂ =0.2216	R ₁ =0.0642, wR ₂ =0.2056	R ₁ =0.0490, wR ₂ =0.1348	R ₁ =0.0491, wR ₂ =0.1409	R ₁ =0.0704, wR ₂ =0.2268	R ₁ =0.0962, wR ₂ =0.2745
Large diff. peak and hole/e Å ⁻³	0.669 and -0.393	1.957 and -0.572	0.660 and -0.511	0.501 and -0.349	1.341 and -1.322	1.849 and -2.242

Table S2. Selected bond lengths (Å) and angles (°) of OTP.

OTP			
N(2)-C(10)	1.336(4)	N(1)-C(5)	1.334(4)
N(2)-C(6)	1.348(4)	C(5)-N(1)-C(1)	116.3(3)
C(34)-N(5)-O(1)	114.0(6)	C(19)-N(4)-C(22)	118.7(3)

Table S3. Selected bond lengths (Å) and angles (°) of FTP-ZnCl₂.

FTP-ZnCl ₂			
Zn(1)-N(3)	2.091(4)	Zn(1)-N(2)	2.196(4)
Zn(1)-N(4)	2.221(4)	N(3)-Zn(1)-N(2)	74.5(1)
N(3)-Zn(1)-N(4)	74.5(1)	N(2)-Zn(1)-N(4)	146.8(1)

Table S4. Selected bond lengths (Å) and angles (°) of FTP-ZnBr₂.

FTP-ZnBr ₂			
-----------------------	--	--	--

Zn(1)-N(2)	2.104(4)	Zn(1)-N(3)	2.205(5)
Zn(1)-N(4)	2.214(4)	N(2)-Zn(1)-N(3)	74.3(2)
N(2)-Zn(1)-N(4)	74.0(2)	N(3)-Zn(1)-N(4)	145.1(2)

Table S5. Selected bond lengths (Å) and angles (°) of **OTP-ZnCl₂**.

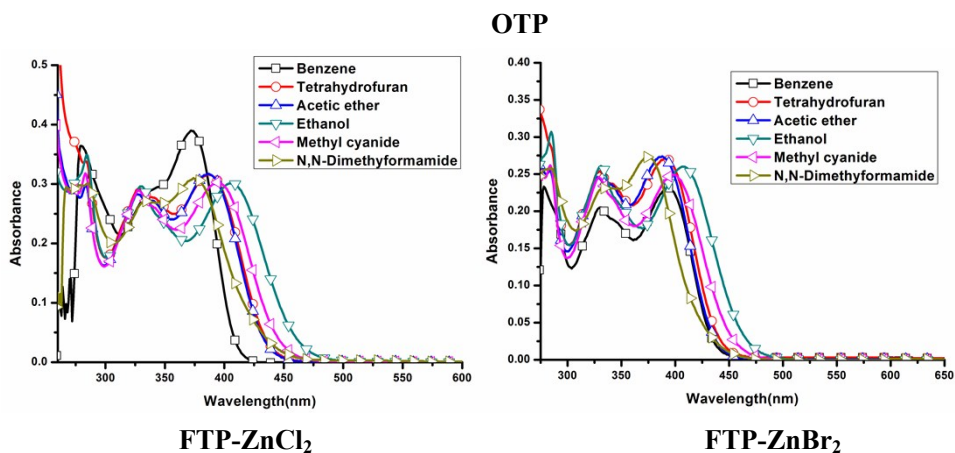
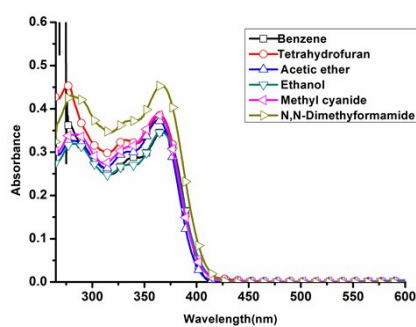
OTP-ZnCl ₂			
Zn(1)-N(4)	2.104(3)	Zn(1)-N(3)	2.202(3)
Zn(1)-N(5)	2.221(3)	N(4)-Zn(1)-N(3)	74.3(1)
N(4)-Zn(1)-N(5)	74.1(1)	N(3)-Zn(1)-N(5)	147.7(1)

Table S6. Selected bond lengths (Å) and angles (°) of **OTP-ZnBr₂**.

OTP-ZnBr ₂			
N(3)-Zn(1)	2.197(1)	N(1)-Zn(1)	2.234(1)
N(2)-Zn(1)	2.097(5)	N(2)-Zn(1)-N(3)	74.4(4)
N(2)-Zn(1)-N(1)	74.5(4)	N(3)-Zn(1)-N(1)	148.3(4)

Table S7. Selected bond lengths (Å) and angles (°) of **OTP-ZnI₂**.

OTP-ZnI ₂			
N(3)-Zn(1)	2.207(5)	N(4)-Zn(1)	2.100(5)
N(5)-Zn(1)	2.213(5)	N(4)-Zn(1)-N(3)	74.8(2)
N(4)-Zn(1)-N(5)	74.2(2)	N(3)-Zn(1)-N(5)	148.3(2)



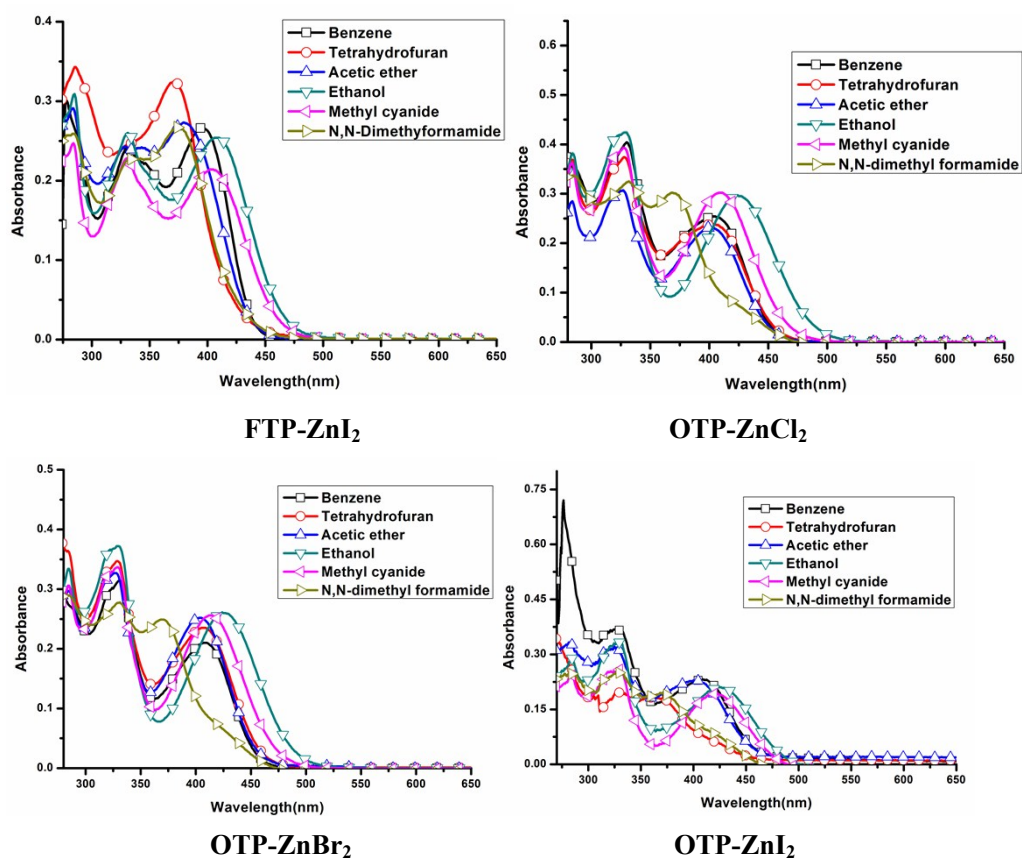


Fig S1. Linear absorption spectra of OTP, FTP-ZnX₂ and OTP-ZnX₂ (X=Cl, Br, I) in different solvents (c=10 μ M).

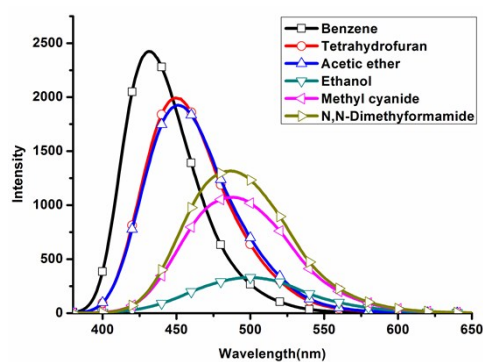
Table S8. The photophysical data of OTP, FTP-ZnX₂ and OTP-ZnX₂ (X=Cl, Br, I) in different solvents.

compound	Solvents	λ_{\max}^{abs} (nm) ^[a]	ϵ_{\max}^b	λ_{\max}^{SPEF} (nm) ^[c]	τ ^[d]	$\Delta\nu$ (nm) ^[e]	ϕ ^[f]
OTP	Benzene	368	3.37	431	1.67	63	0.46
	Tetrahydrofuran	364	3.86	449	2.86	85	0.41
	Ethyl acetate	363	3.74	451	2.39	88	0.42
	Ethanol	366	3.48	498	1.77	132	0.10
	Acetonitrile	363	3.87	489	4.26	126	0.28
	DMF	367	4.54	486	4.46	119	0.29
FTP-ZnCl ₂	Benzene	389	3.90	473	2.88	86	0.22
	Tetrahydrofuran	387	3.17	515	5.04	128	0.19
	Ethyl acetate	386	3.16	517	4.92	131	0.20

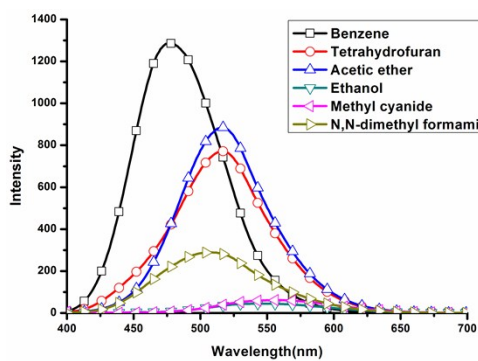
	Ethanol	405	3.04	551	2.02	146	0.02
	Acetonitrile	394	3.05	555	2.91	161	0.02
	DMF	374	3.10	516	5.41	142	0.11
FTP-ZnBr ₂	Benzene	393	2.32	473	2.66	80	0.49
	Tetrahydrofuran	391	2.74	517	4.22	126	0.23
	Ethyl acetate	389	2.75	518	4.10	129	0.25
	Ethanol	408	2.63	551	1.83	143	0.02
	Acetonitrile	399	2.49	559	1.16	160	0.02
	DMF	376	2.74	508	5.43	132	0.07
FTP-ZnI ₂	Benzene	396	2.64	472	1.91	76	0.03
	Tetrahydrofuran	371	3.25	462	3.35	91	0.25
	Ethyl acetate	379	2.73	517	2.75	138	0.11
	Ethanol	408	2.54	554	1.72	146	0.01
	Acetonitrile	404	2.14	563	-	159	-
	DMF	374	2.67	506	4.03	132	0.10
OTP-ZnCl ₂	Benzene	405	2.54	516	3.86	111	0.17
	Tetrahydrofuran	403	2.39	535	3.21	132	0.05
	Ethyl acetate	401	2.31	535	2.72	134	0.04
	Ethanol	424	2.97	565	-	141	-
	Acetonitrile	409	3.02	574	-	165	-
	DMF	369	3.02	492	4.68	123	0.22
OTP-ZnBr ₂	Benzene	408	2.10	518	3.52	110	0.13
	Tetrahydrofuran	406	2.35	536	2.72	130	0.04
	Ethyl acetate	404	2.52	535	2.43	131	0.03
	Ethanol	424	2.61	560	-	136	-
	Acetonitrile	413	2.56	575	-	162	-
	DMF	370	2.49	490	4.66	120	0.25

OTP-ZnI ₂	Benzene	406	2.23	514	2.78	108	0.08
	Tethydrofuran	371	2.81	528	3.07	157	0.05
	Ethyl acetate	404	2.30	532	2.14	128	0.03
	Ethanol	423	2.10	553	1.70	130	-
	Acetonitrile	420	1.94	582	-	162	-
	DMF	369	1.95	492	4.57	123	0.05

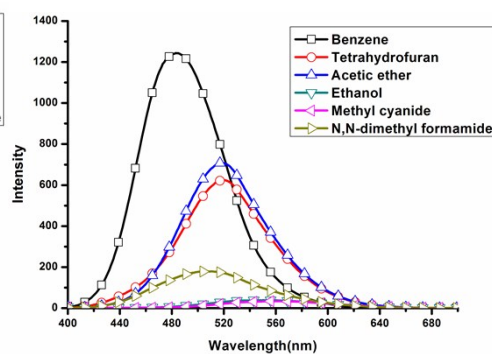
[a] Peak position of the longest absorption band. [b] Molar absorbance in $10^4 \text{ mol}^{-1} \text{ L cm}^{-1}$. [c] Peak position of one-photon fluorescence spectra, excited at the absorption maximum. [d] Fluorescence lifetime (ns). [e] Stokes' shift in nm. [f] Quantum yields determined by using fluorescein as standard



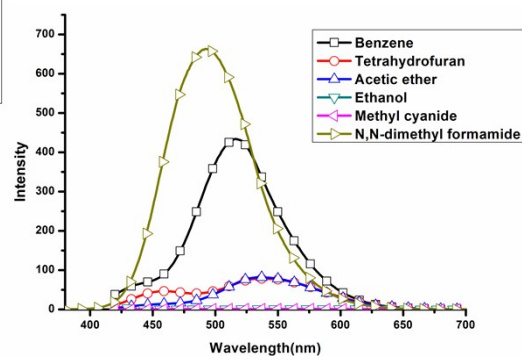
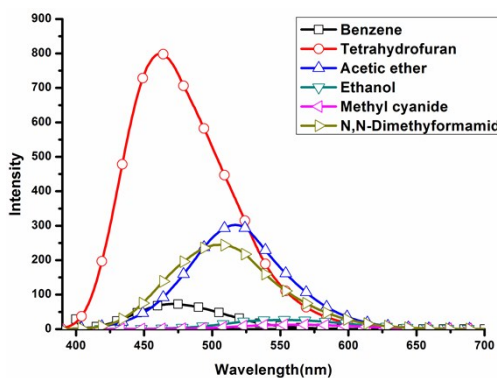
OTP



FTP-ZnCl₂



FTP-ZnBr₂



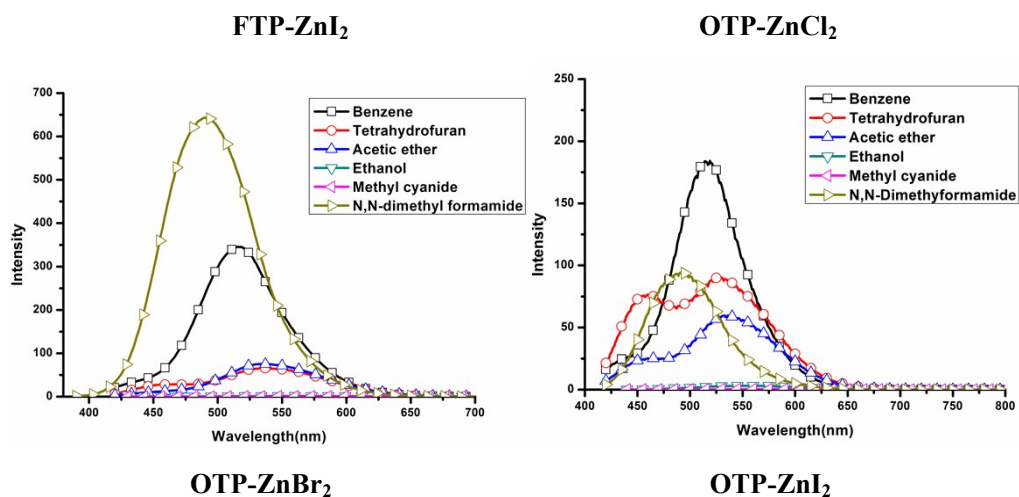


Fig S2. One-photon fluorescence spectra of OTP, FTP-ZnX₂ and OTP-ZnX₂ (X=Cl, Br, I) in different solvents (c=10 μM).

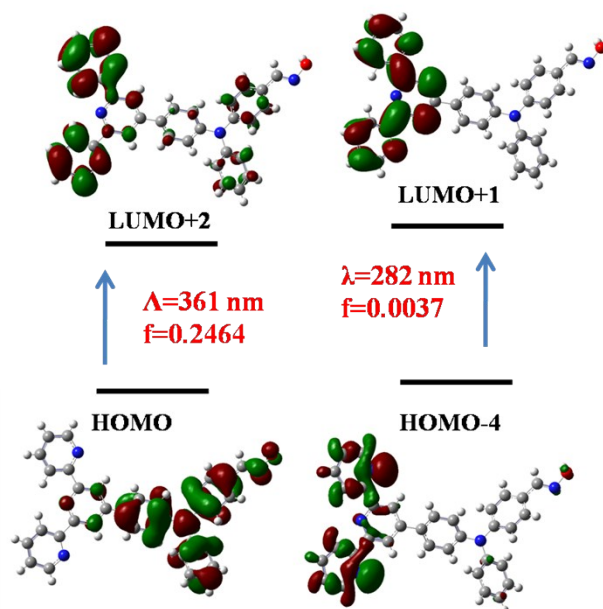


Fig S3. Molecular orbital energy diagram of OTP.

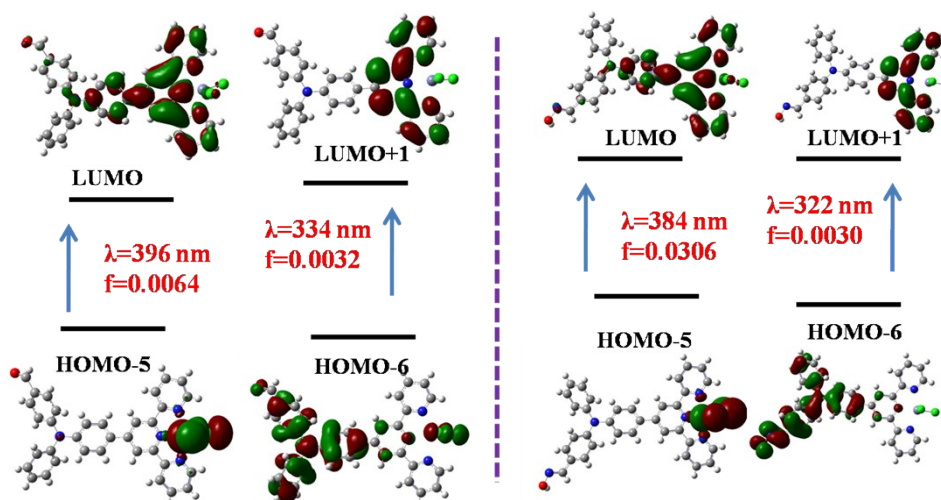


Fig S4. Molecular orbital energy diagram of FTP-ZnCl₂ (left) and OTP-ZnCl₂ (right).

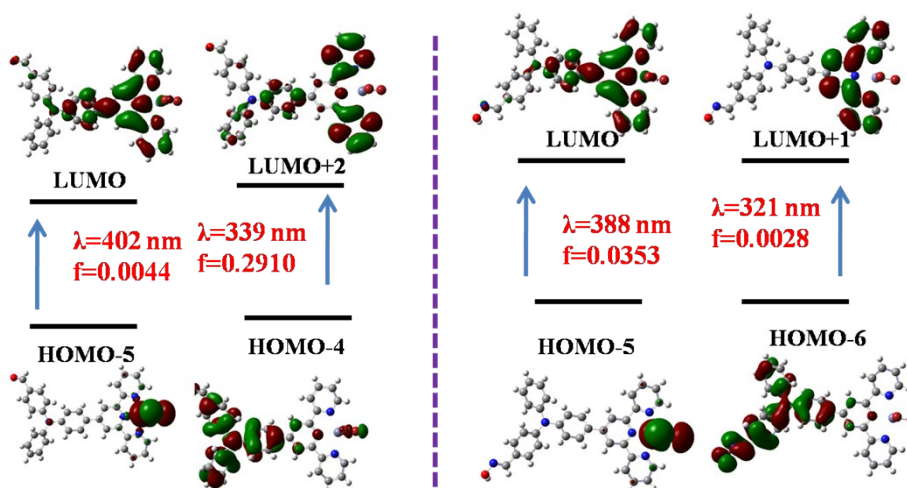


Fig S5. Molecular orbital energy diagram of FTP-ZnBr₂ (left) and OTP-ZnBr₂ (right).

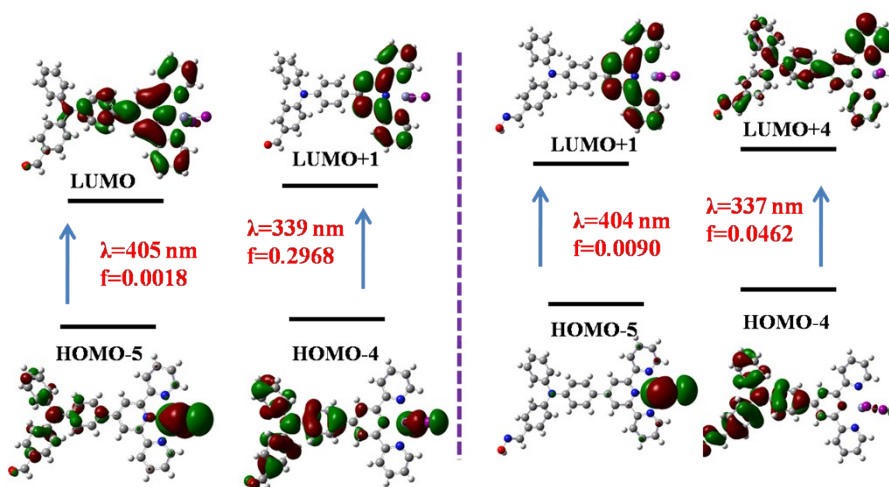


Fig S6. Molecular orbital energy diagram of FTP-ZnI₂ (left) and OTP-ZnI₂ (right).

Table S9. Calculated leaner absorption properties (nm), excitation energy (eV), oscillator strengths and major contribution for all compounds.

Cmpd	ΔE_1 [a]	λ [nm] ^[b]	Oscillator strengths	Nature of the transition
OTP	3.44	361	0.2464	136(H) \rightarrow 139(L+2)(0.70)
	4.39	282	0.0037	132(H-4) \rightarrow 138(L+1)(0.55)
FTP-ZnCl ₂	3.12	396	0.0064	140(H-5) \rightarrow 146(L)(0.68)
	3.70	334	0.0032	139(H-6) \rightarrow 147(L+1)(0.68)
FTP-ZnBr ₂	3.08	402	0.0044	140(H-5) \rightarrow 146(L)(0.69)
	3.63	339	0.2910	141(H-6) \rightarrow 148(L+2)(0.50)
FTP-ZnI ₂	3.06	405	0.0018	140(H-5) \rightarrow 146(L)(0.51)
	3.65	339	0.2968	141(H-4) \rightarrow 147(L+1)(0.66)
OTP-ZnCl ₂	3.22	384	0.0306	144(H-5) \rightarrow 150(L)(0.69)
	3.84	322	0.0030	143(H-6) \rightarrow 151(L+1)(0.69)
OTP-ZnBr ₂	3.19	388	0.0353	144(H-5) \rightarrow 150(L)(0.70)
	3.86	321	0.0028	143(H-6) \rightarrow 151(L+1)(0.50)
OTP-ZnI ₂	3.06	404	0.0090	144(H-5) \rightarrow 151(L+1)(0.69)
	3.67	337	0.0462	145(H-4) \rightarrow 154(L+4)(0.44)

[a] The energy gap of the single-photon absorption band. [b] Peak position of the maximum absorption band.

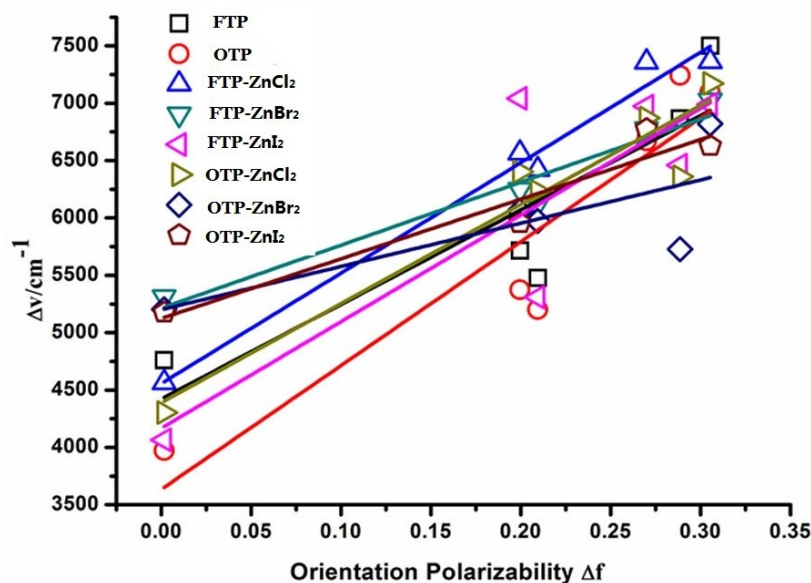


Fig S7. Lippert-Mataga plots for FTP, OTP, FTP-ZnX₂ and OTP-ZnX₂ (X=Cl, Br, I).

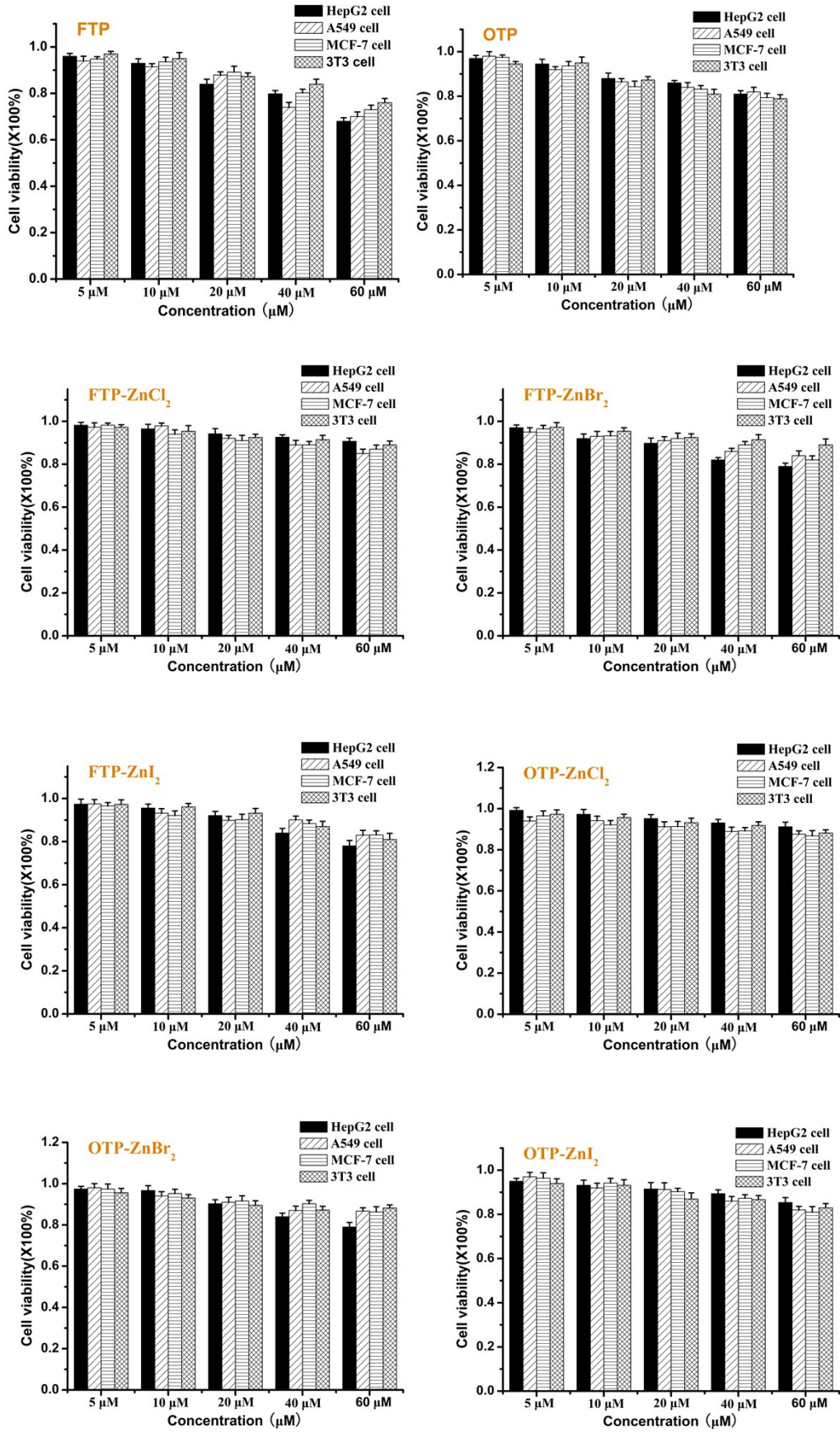


Fig S8. Cytotoxicity data results obtained from the MTT assay.

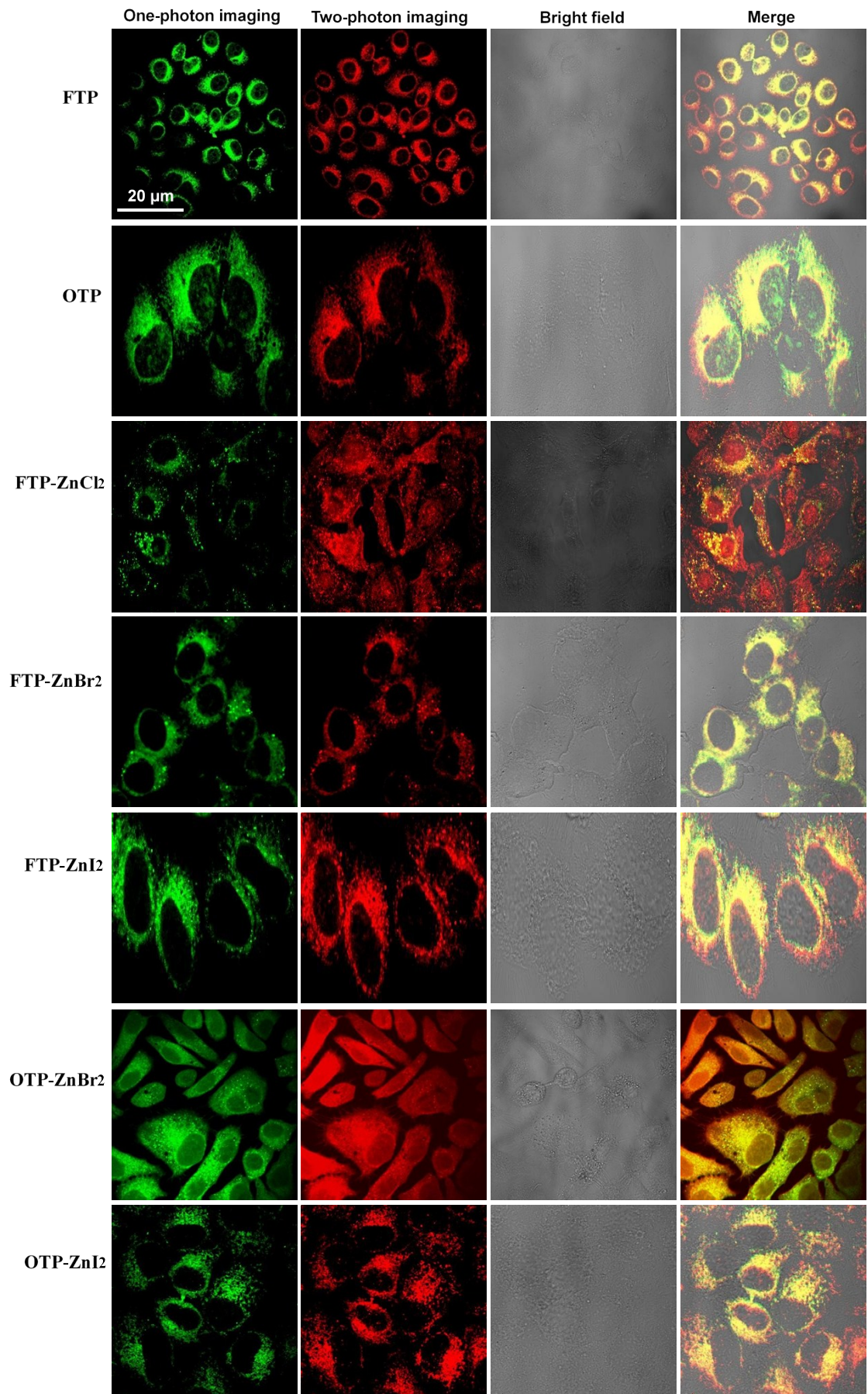


Fig S9. One- and two-photon images of HepG2 cells incubated with **FTP**, **OTP** and their ZnX_2 ($\text{X}=\text{Cl}$, Br , I) complexes ($30 \mu\text{M}$, 30 min) at 37°C . One-photon excited wavelength: 405 nm ; emission filter: $510\text{-}570 \text{ nm}$. Two-photon excited wavelength: 820 nm ; emission filter: $520\text{-}580 \text{ nm}$.

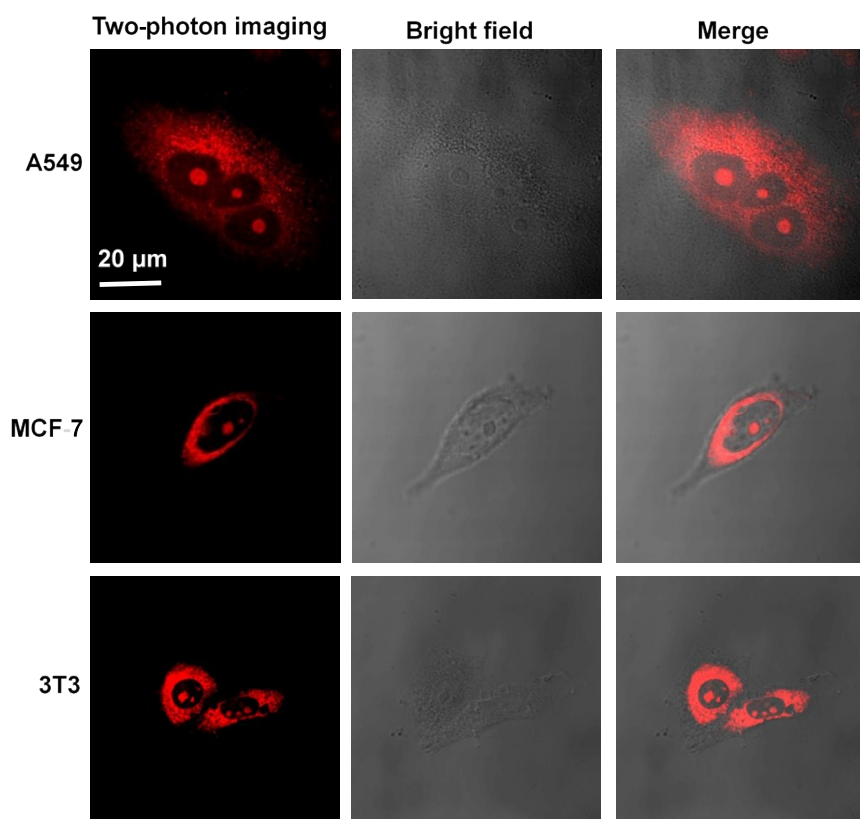


Fig S10. Two-photon imaging of A549, MCF-7 and 3T3 cells stained with $30 \mu\text{M}$ **OTP-ZnCl₂** for 30 min .

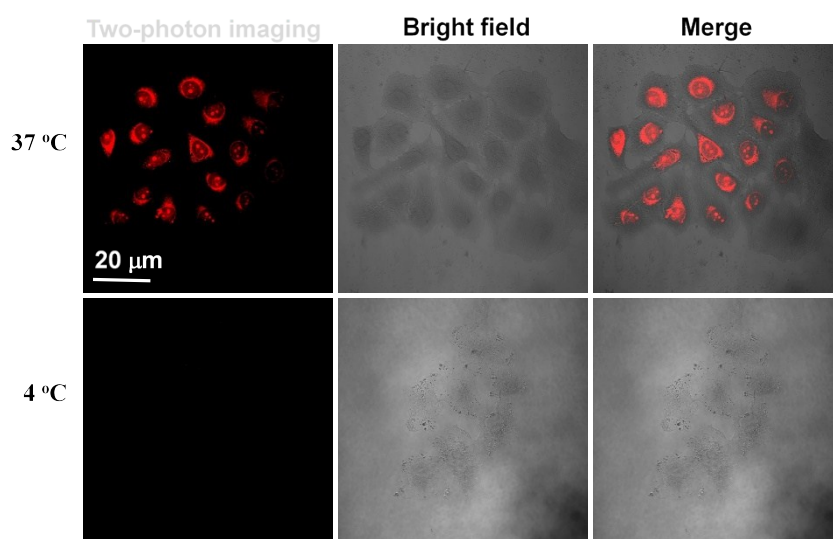


Fig S11. Two-photon image of HepG2 cells incubated with **OTP-ZnCl₂** at 37°C and 4°C for 30 minutes .

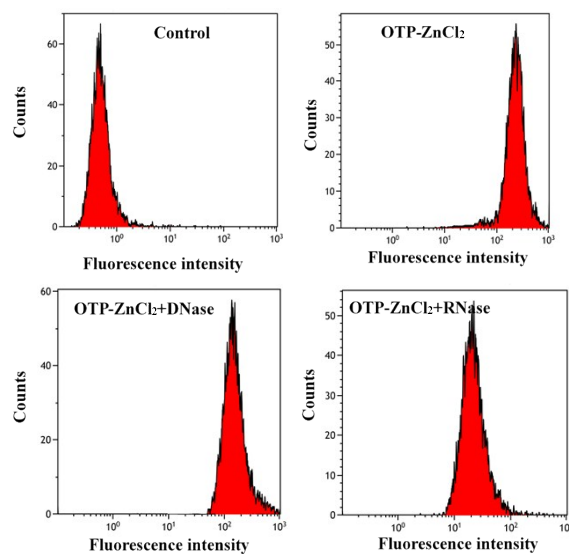


Fig S12. HepG2 cells by flow cytometry upon incubating the cells with **OTP-ZnCl₂** for 30 min before and after treatment with DNase and RNase for 2 h.

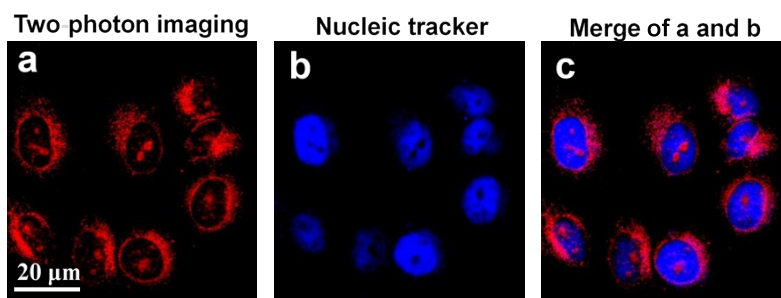


Fig S13. Live cell counterstain with Hoechst 33342. Two-photon imaging of HepG2 cells stained with **OTP-ZnCl₂** (30 μM) (a) for 30 min followed by staining with 1 μM Hoechst 33342 (b) for 15 min. (c) Merge image of **OTP-ZnCl₂** and Hoechst 33342. Scale bar= 20 μm.

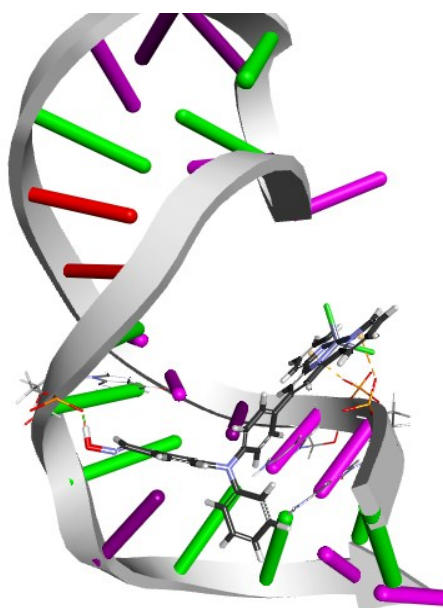


Fig S14. The view of the interaction between **OTP-ZnCl₂** with RNA fragment.

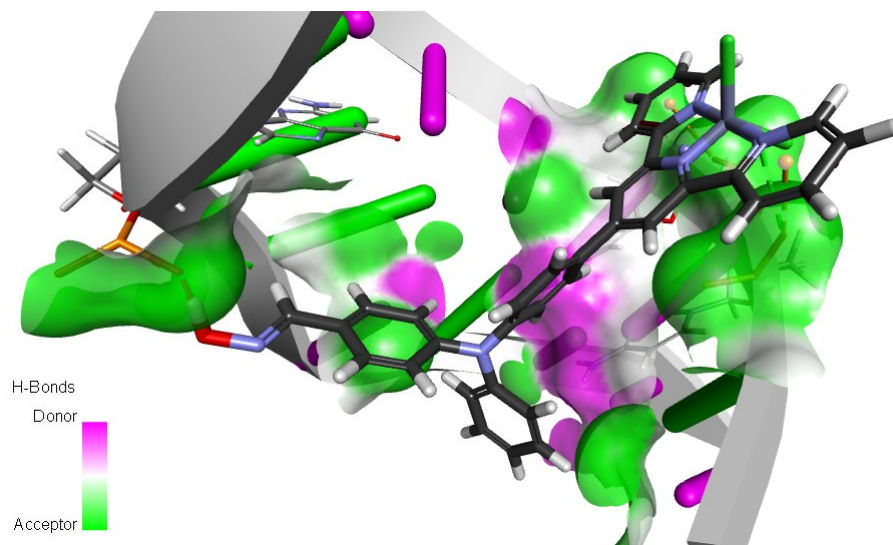


Fig S15. The view of the hydrogen bond interaction between **OTP-ZnCl₂** with the surface of RNA fragment.

References

- [1] J. N. Demas and G. A. Crosby, The measurement of photoluminescence quantum yields. *J. Phys. Chem.*, 1971, **75**, 991-24.
- [2] C. Xu and W. W. Webb, Measurement of two-photon excitation cross-sections of molecular fluorophores with data from 690 to 1050nm. *J. Opt. Soc. Am. B.*, 1996, **13**, 481-491.
- [3] M. A. Albota, C. Xu and W. W. Webb, Two-photon fluorescence excitation cross-sections of biomolecular probes from 690 to 960nm. *Applied. Optics.*, 1998, **37**, 7352-7356.
- [4] J. Liu, Q. Zhang, H. J. Ding, J. Zhang, J. Y. Tan, C. K. Wang, J. Y. Wu, S. L. Li, H. P. Zhou, J. X. Yang and Y. P. Tian, *Sci. China. Chem.*, 2013, **56**, 1315-1324.
- [5] G. M. Sheldrick, SHELXTL97, Program for crystal structure solution; University of Göttingen: Göttingen. Germany. 1997.
- [6] M. J. Frisch, G. W. Trucks, H. B. Schlegel, G. E. Scuseria, M. A. Robb, J. R. Cheeseman, et al. Gaussian 03 (Revision B.04), Gaussian, Inc. Wallingford, CT, 2004.